



## Preparation, characterization and coagulation performance of a composite coagulant formed by the combination of polyferric sulfate (PFS) and $Ce^{3+}$

Mei Liu\*, Pengfei Zhu, Yao Ran, Yanjun Chen, Lina Zhou

School of Chemistry and Chemical Engineering, Southwest Petroleum University, Chengdu 610500, China, Tel. +86 28 83037321; Fax: +86 28 83037305; emails: [verababy620@126.com](mailto:verababy620@126.com) (M. Liu), [pengfeizhu@aliyun.com](mailto:pengfeizhu@aliyun.com) (P. Zhu), [66978996@qq.com](mailto:66978996@qq.com) (Y. Ran), [2421800600@qq.com](mailto:2421800600@qq.com) (Y. Chen), [972682155@qq.com](mailto:972682155@qq.com) (L. Zhou)

Received 19 December 2014; Accepted 30 May 2015

### ABSTRACT

A series of composite coagulants (Ce-PFS) with different Ce/Fe molar ratios or adding order of  $Ce^{3+}$  were prepared. FTIR, UV spectra, and XRD were employed to characterize the samples and Fe-Ferron time-by-time complexation colorimetry method was used to analyze their Fe species. The coagulation performance of the coagulants was evaluated through their decolorization rate for treating direct sky blue or direct fast claret dye wastewater. The results showed that the new bond of Ce–OH–Fe was formed between  $Ce^{3+}$  and polyferric sulfate (PFS), leading to the formation of a new compound.  $Ce^{3+}$  not only increased the molecular weight of the coagulant and the accumulation charge of the single particle, but also promoted the conversion of Fe(a) to Fe(b) and Fe(c). In addition, the performance of Ce-PFS was superior to PFS. The decolorization rate of Ce-PFS ( $Ce^{3+}$  was added after  $NaClO_3$ , Ce/Fe molar ratio was 0.6%) for treating direct sky blue could reach up to 98% at the dosage of 75 mg/L. Meanwhile, its decolorization rate for treating direct sky blue was higher than that of direct fast claret dye wastewater under the same condition.

*Keywords:* Composite coagulant; Polyferric sulfate;  $Ce^{3+}$ ; Dye wastewater

### 1. Introduction

Dye wastewater has a serious threat to the surface and underground water resources due to its high amount of suspended solids, color intensity and chemical oxygen demand [1]. The conventional purification of water/wastewater mainly includes the processes of adsorption–flocculation, physicochemical coagulation–flocculation, membrane filtration, activated carbon adsorption and biological treatment [2–5]. Compared to the other treatment methods, flocculation technology exhibits some advantages such as

brief process, convenient operation, good biodegradability of dyeing wastewater, and so on [6]. For flocculation technology, inorganic polymeric coagulants are becoming popular for water treatment because they contain more effective coagulation species that can produce better coagulation performance than other water treatment reagents [7]. And polyferric sulfate (PFS), which is considered as a better inorganic polymer coagulant over other hydrolysing metallic salts, is widely used as reagent in dye wastewater treatment due to its better performance, lower cost, and wider range of pH [8–10]. Meanwhile, ferric ions can play an important role in removing of the color

\*Corresponding author.

[11]. Therefore, there are many investigations focused on improving the performance and exploring the use of PFS.

The coagulation efficiency of PFS can be improved by adding modifier to produce new composite coagulant, including Al ions, Si species, Ti ions and other metal ions [2,12,13]. In principle, an effective modifier, usually carry high cationic charge, can result in higher coagulation efficiency of the composite coagulant [14–18]. Rare earth metals are widely used in various technological devices, including superconductors, catalysts, coagulants, and so on [19,20]. Among all rare earth metals, cerium is the most abundant element.  $Ce^{3+}$  has high cationic charge and complexing ability [21]. It could promote the performance of the coagulant on treating wastewater. But it is a pity that  $Ce^{3+}$  is poor explored. Therefore, greater efforts are required to investigate PFS coagulant with  $Ce^{3+}$  as modifier. Based on the preliminary results, this article is to give a study on the preparation, characterization and coagulation performance of PFS composited with  $Ce^{3+}$ .

## 2. Materials and methods

### 2.1. Materials

The dye wastewater used in this study was prepared using direct sky blue or direct fast claret as the raw material. Both the concentration of the two kinds of dye wastewater was 50 mg/L. These two dyes, without further purification, were obtained from Tianjin Yishang Chemical Materials Company, China. Their structures are shown in Fig. 1. All other chemical reagents, which were analytically pure, and

the de-ionized water with conductivity lower than  $0.5 \mu\text{S}/\text{cm}$  were used to prepare all the solutions.

The coagulation experiment was conducted in a water bath with magnetic stirrer (Jiangsu Guohua Co., China). V-1800 visible spectrophotometer (Shanghai Meipuda Co., China) was used to measure the decolorization rate of the dye wastewater and determinate Fe polymeric species of the coagulants.

The X'Pert Pro X-ray diffractometer (Panalytical, Holland), WQF-520 FTIR spectrophotometer (Beijing Ruili, China), and UV-1800 spectrophotometer (Shimadzu, Japan) were used to characterize the structure of the coagulants.

### 2.2. Preparation of the coagulants

Three kinds of composite coagulants (Ce-PFS(A), Ce-PFS(B), and Ce-PFS(C)) were prepared according to the addition order of raw materials.

For Ce-PFS(A), the  $Ce(NO_3)_3 \cdot 6H_2O$  was added after  $NaClO_3$ . The detail of preparation of Ce-PFS(A) was as follows: Firstly, 28 g  $FeSO_4 \cdot 7H_2O$  and 18 mL water were added into a 150-mL beaker, after stirring at  $60^\circ\text{C}$  for several minutes,  $FeSO_4$  aqueous solution was obtained; then, 2.5 mL concentrated sulfuric acid was added slowly into the  $FeSO_4$  aqueous solution under the stirring, followed by 4.5 g  $NaClO_3$  powder was added into the mixture solution and agitated for 30 min, PFS was obtained. At last,  $Ce(NO_3)_3 \cdot 6H_2O$  powder was added into PFS. After stirring for 30 min and holding for 1 h at  $60^\circ\text{C}$  and aging for 24 h at room temperature, liquid composite coagulant Ce-PFS(A) was obtained. The liquid samples were dried at  $60^\circ\text{C}$  in vacuum drying oven until the solid samples were

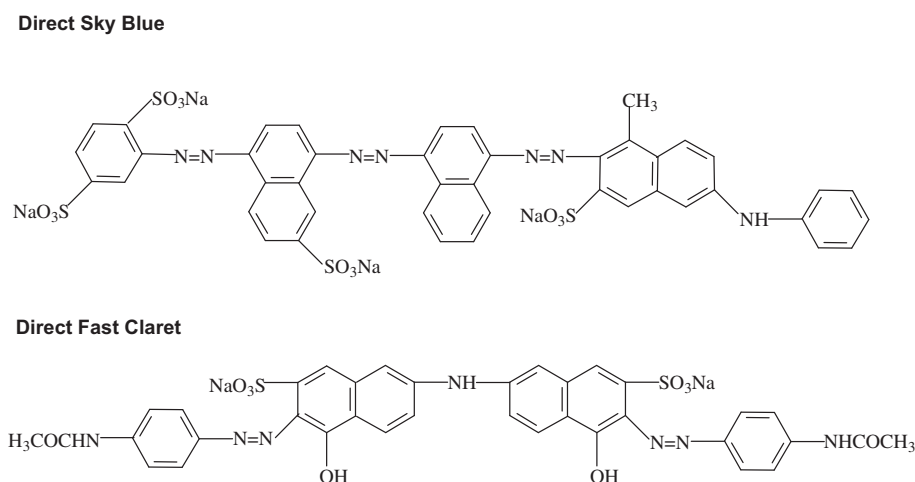


Fig. 1. Chemical structure of the two dyes.

obtained. A series of solid Ce-PFS(A) were prepared by changing the molar ratio of Ce/Fe in Ce-PFS(A), such as 0.0, 0.2, 0.4, 0.6, 0.8 and 1.0%.

For Ce-PFS(B),  $\text{Ce}(\text{NO}_3)_3 \cdot 6\text{H}_2\text{O}$  was added simultaneously with  $\text{NaClO}_3$ . The detail of preparation of Ce-PFS(B) was similar with that of Ce-PFS(A).

For Ce-PFS(C),  $\text{Ce}(\text{NO}_3)_3 \cdot 6\text{H}_2\text{O}$  was added after PFS aged for 24 h. The mixture solution was stirred at 60°C for 30 min, then aged for 24 h and dried. Ce-PFS (C) coagulant was prepared.

### 2.3. Coagulation experiments

Coagulation tests were performed in beakers using simulated dye wastewater containing direct sky blue or direct fast claret. At room temperature and the initial pH of the dye wastewater, 200 mL test wastewater was placed in a 500-mL beaker. Under stirring at 200 rpm, coagulant reagent was added. Then, the dye wastewater was stirred at 120 rpm for 5 min and at 80 rpm for 10 min, respectively. At last, it was placed for 30 min. The supernatant sample was extracted for measurement the absorbance at its maximum absorption peak with pure water as reference solution. Then, according to the standard curve of the dye, the decolorization rate was calculated using  $D = [(C_0 - C_1)/C_0] \times 100\%$ , where  $C_0$  and  $C_1$  were the absorbance of the initial solution and the supernatant sample, respectively.

### 2.4. Characterization of the coagulants

XRD was measured for the determination of crystalline phases in solid coagulants using X-ray diffractometer with Cu  $K\alpha$  radiation in the range of 5°–60° ( $2\theta$ ), at a scan rate of 0.02 °/s. The solid coagulants were analyzed by FTIR with the WQF-520 FTIR spectrophotometer and potassium bromide pellet technique. The liquid coagulants were serially diluted, then analyzed by UV spectra with the UV-1800 spectrophotometer, and the spectra were recorded in the range of 200–800 nm. At the same time, the species distribution of Fe species was determined by the application of Fe-Ferron time-by-time complexation colorimetry method [22]. The ferron reagent (8-hydroxyl-iodoquinoline-5-sulfonic acid) can form complexes with ferric ions. According to the difference of the reaction rate, the species of Fe can be generally classified in three categories as Fe(a) (oligomers, which react with ferron in 1 min), Fe(b) (polymers with increasing reaction time), and Fe(c) (precipitated species, i.e.  $\text{Fe}(\text{OH})_3(\text{s})$  particles, which do not react with ferron) [23]. The absorbance of the solution with

different reaction time was measured using V-1800 visible spectrophotometer at 600 nm with blank solution as reference solution. Combining with the standard curve of ferric ions, the concentration of Fe(a) was determined from the absorbance reading taken 1 min after mixing of the ferron reagent and the sample. The concentration of Fe(b) was determined from the difference between the absorbance at 24 h and 1 min. And the content of Fe(c) was obtained by subtracting Fe(a) and Fe(b) from the total iron concentration.

## 3. Results and discussion

### 3.1. Characterization of coagulants

#### 3.1.1. XRD analysis

Fig. 2 illustrates the XRD spectra of PFS and Ce-PFS(A) samples with different Ce/Fe molar ratios, and the analysis results showed that there are  $\text{Fe}_2(\text{SO}_4)_3(\text{H}_2\text{O})_{11}$ ,  $\text{Fe}_2(\text{SO}_4)_3(\text{H}_2\text{O})_9$ ,  $\text{Fe}_2(\text{SO}_4)_3$ ,  $\text{Fe}(\text{OH})\text{SO}_4(\text{H}_2\text{O})$ ,  $\text{Fe}(\text{OH})\text{SO}_4(\text{H}_2\text{O})_2$ , and other crystals [24]. A new peak at 12.0° was observed for Ce-PFS(A) samples, suggesting that the composite coagulant was formed at some extent.

The XRD spectra also showed that the intensity of the diffraction peaks of Ce-PFS(A) was higher than that of PFS. Moreover, when Ce/Fe molar ratios were different, the intensity of the diffraction peak of Ce-PFS(A)s were different. As the Ce/Fe molar ratio is increasing, the intensity decreased firstly, and increased afterward, it reached its minimum value when the mole ratio of Ce/Fe was 0.6%. It indicated that an appropriate amount of  $\text{Ce}^{3+}$  could lead to lower crystallinity, better dispersion and higher ratio of the undefined structure of the products. It could also conclude that the molecular weight of the polymer increased after the inducing of  $\text{Ce}^{3+}$ , therefore, the chain segment motion became worse and resulted in the limitation of molecule diffusion and ordination to crystal, and then the lower crystallinity was obtained.

#### 3.1.2. FTIR spectra analysis

Fig. 3 displays the FTIR spectra of PFS and composite coagulants ( $r = 0.6\%$ ). As shown in Fig. 3, it was found that there are strong absorption peaks at 3,600–3,100 and 1,640  $\text{cm}^{-1}$ , which are assigned to the stretching vibration of  $-\text{OH}$  and vibration of water absorbed. Meanwhile, the peaks at 856 and 471  $\text{cm}^{-1}$  are regarded as the symmetrical stretching vibrations of  $\text{Fe}-\text{OH}-\text{Fe}$  and the vibrations of  $\text{Fe}-\text{O}$ , respectively [25,26]. This suggested that the prepared coagulant

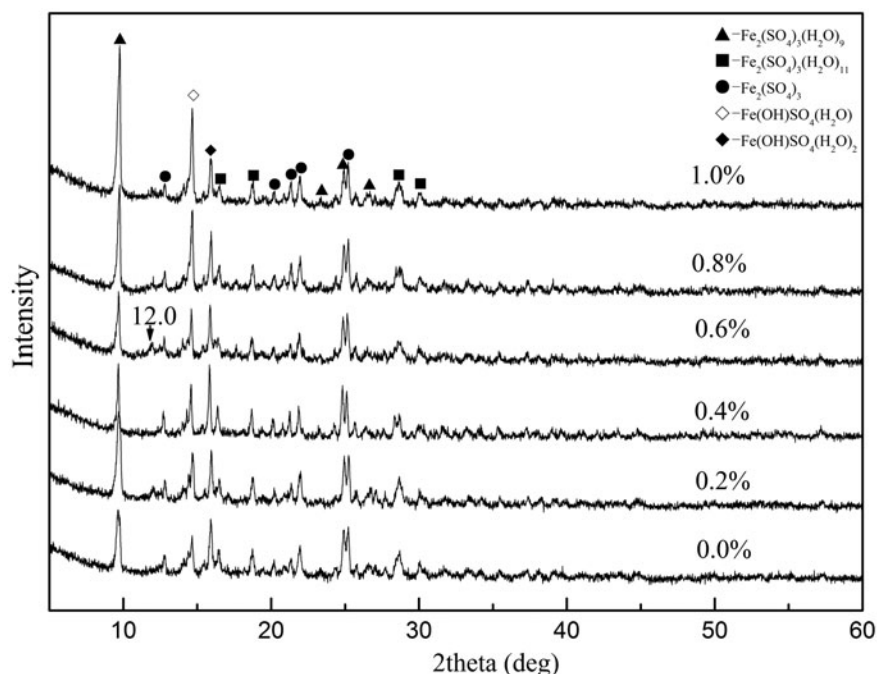


Fig. 2. XRD spectra of PFS and Ce-PFS(A) with different Ce/Fe molar ratios.

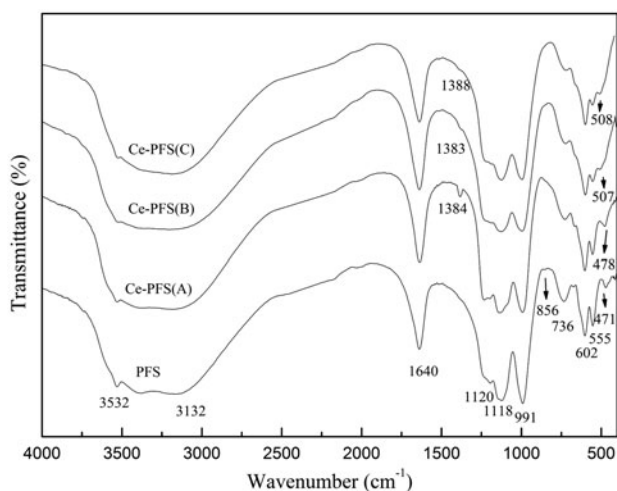


Fig. 3. FTIR spectra of PFS and Ce-PFS ( $r = 0.6\%$ ) with different adding modifier orders.

was a kind of polymer formed by the OH bridges. No significant changes on the peak shapes of PFS and Ce-PFS were observed. But, there was a new peak at about  $1,384\text{ cm}^{-1}$  of Ce-PFS, which may be attributed to the formation of the new bond Ce–OH–Fe between  $\text{Ce}^{3+}$  and PFS. It was another proof that Ce-PFS contained new chemical species rather than a simple mixture of the raw materials. The addition of  $\text{Ce}^{3+}$  might

increase the molecular weight of the coagulant and the accumulation charge of the single particle, which could play useful roles of bridging and adsorption, charge neutralization, and co-precipitation netting.

Meanwhile, the peak shapes of the Ce-PFS samples were almost the same, but the intensity of the absorption peak at  $1,383\text{ cm}^{-1}$  of Ce-PFS(B) and  $1,388\text{ cm}^{-1}$  of Ce-PFS(C) was weaker than that of Ce-PFS(A). This illustrated that the addition order of  $\text{Ce}^{3+}$  could influence the formation of Ce–OH–Fe. The addition order of Ce-PFS (B) and Ce-PFS(C) were disadvantageous to obtain the Ce-PFS composite coagulant. Compared to the PFS sample, the blueshift of absorption peak at about  $471\text{ cm}^{-1}$  of Ce-PFS samples was observed. It mainly resulted from the stronger coordination capabilities of  $\text{Fe}^{3+}$  than  $\text{Ce}^{3+}$ , which enhanced the bond of Fe–O in Ce–OH–Fe. While for Ce-PFS(A), the position of this peak changed a little. It might be due to that the increase of  $\text{Ce}^{3+}$  promoted the substitution of  $\text{Fe}^{3+}$ , and even caused the formation of some Ce–OH–Ce. Thereby, the blueshift became weak.

### 3.1.3. UV spectra analysis

The UV absorption spectra of PFS and Ce-PFS(A) ( $r = 0.6\%$ ) are presented in Fig. 4. It was evident that UV absorption spectra of the two samples was similar to each other in shape, but the peak of Ce-PFS(A) was

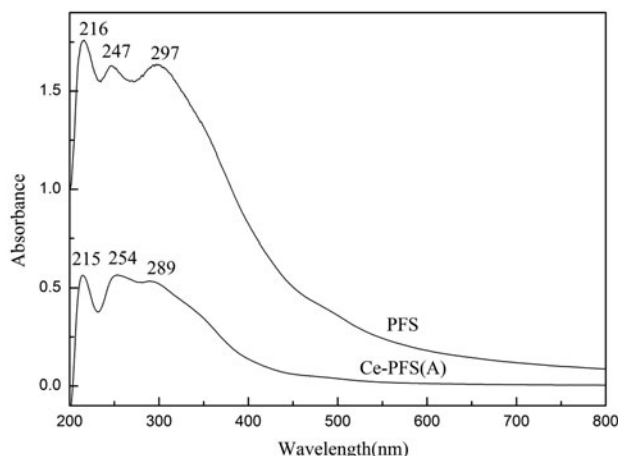


Fig. 4. UV absorption spectra of PFS and Ce-PFS(A) ( $r = 0.6\%$ ).

smoother than that of PFS. This was attributed to the increase of the solvent polarity because of the addition of  $\text{Ce}(\text{NO}_3)_3$ . Meanwhile, the absorption peaks intensity of Ce-PFS(A) was weaker than that of PFS. It is probably because the formation of Ce–OH–Fe affected the absorption of the solution. In addition, the peaks of PFS at 216, 247, and 297 nm are regarded as the absorption of  $\text{SO}_4^{2-}$ ,  $\text{Fe}^{3+}$ , and  $\text{FeOH}^{2+}$ , respectively [27,28]. Fig. 4 also shows shifting of the corresponding peak from 247 nm of PFS to 254 nm of Ce-PFS(A). This red shift in peak was attributed to the reduced symmetry of the original octahedron-field of  $\text{Fe}^{3+}$  caused by the strong interaction between  $\text{Ce}^{3+}$  and OH of the PFS. The peak observed at 297 nm of PFS shifted to 289 nm, which was mainly attributed to the increase of  $\text{Fe}^{3+}$  in the solution resulted from some exchange from  $\text{Fe}^{3+}$  in Fe–OH–Fe by  $\text{Ce}^{3+}$ .

### 3.1.4. Determination of Fe species in the coagulants

Table 1 illustrates that the distribution of Fe species of PFS and Ce-PFS(A). In comparison with the relevant values of pure PFS, the content of Fe(a) was reduced while the content of Fe(c) was increased in Ce-PFS(A). The bond of Ce–OH–Fe was formed

Table 1  
The distribution of Fe species of PFS and Ce-PFS(A)

Ce/Fe	0.0%	0.2%	0.4%	0.6%	0.8%	1.0%
Fe(a) (%)	80.30	75.30	66.90	54.70	55.10	57.60
Fe(b) (%)	14.60	18.73	22.90	30.00	28.07	24.92
Fe(c) (%)	5.10	5.97	10.20	15.30	16.83	17.48

between  $\text{Ce}^{3+}$  and PFS, which in turn lead to the formation of complex compounds, thus the Fe(a) species reduced.

Additionally, with the increase of Ce/Fe ratio, the degree of Fe(b) increased and then decreased, and it reached the maximum value when  $r = 0.6\%$ . It was reported that Fe(b) plays the major role in the process of the flocculation [22]. The flocculation may be improved as the content of Fe(b) increased. This was correspondent with the results of the coagulation experiments afterward. Meanwhile, the change of the Fe(b) indicated that the presence of  $\text{Ce}^{3+}$  itself would affect the distribution of Fe species in the solution, and  $\text{Ce}^{3+}$  rose the content of Fe(b), which promoted the flocculation effect. It could be concluded that  $\text{Ce}^{3+}$  influenced the hydrolysis of  $\text{Fe}^{3+}$ , and it promoted the conversion of Fe(a) to Fe(b) and Fe(c). And the high percentage of Fe (c) was related with the stability of the coagulants [17].

## 3.2. Coagulation performance

### 3.2.1. Effect of Ce/Fe molar ratio on decolorization rate

Six Ce-PFS(A) coagulants with different compositions were used to treat direct sky blue dye wastewater. Fig. 5 shows the decolorization rate of the dye wastewater when the dosage of coagulant was 50 mg/L. As shown in Fig. 5, the coagulation performance was different along with the Ce/Fe mole ratio. When Ce/Fe mole ratio was in the range from 0 to 0.6%, the performance of Ce-PFS(A) increased with it. It can be suggested that the addition of  $\text{Ce}^{3+}$  increased the molecular weight and positive charge of the composite, eventually

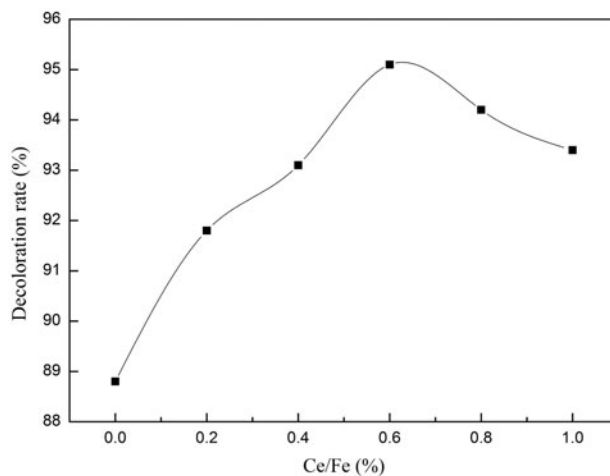


Fig. 5. Coagulation performance of Ce-PFS(A) with different Ce/Fe mole ratios.

leading to the enhancement of co-precipitation netting, bridging, and adsorption. When Ce/Fe mole ratio was 0.6%, Ce-PFS(A) had the best performance, which ascribed to the greatest Fe(b) concentration of the coagulant. Meanwhile,  $Ce^{3+}$  and  $Fe^{3+}$  played a synergistic action and made the compounds pose higher positive charge, which could strengthen the bridging between metallic ion and the negative charge group of direct sky blue [23]. However, the decolorization rate reduced when the Ce/Fe mole ratio continued to increase. This could be attributed to that high amount of  $Ce^{3+}$  might cause precipitation in solution. As a result of the work mentioned above, the molar ratio of Ce/Fe was one of the main factors affecting the performance of the coagulants.

### 3.2.2. Effect of dye species and addition order of $Ce^{3+}$ on decolorization rate

Fig. 6 presents the decolorization rate for treating direct sky blue or direct fast claret dye wastewater with PFS and Ce-PFS ( $r = 0.6\%$ , the dosage of the reagent was 50 mg/L). As shown in Fig. 6, it was found that all the decolorization rates could reach to be 83% although the dye types were different. The presence of the metallic ions of the coagulants and azo  $\pi$ -bond of the dye facilitated the formation of the flocs, through the bridging and adsorption formation mechanism. Meanwhile, there was ligand exchange of surface OH groups of the coagulant and pigment-bearing anion of the dye.

It was also found that the decolorization rate of the coagulants for treating direct sky blue was higher than that of direct fast claret. On the one hand, the different molecular structures resulted in the different

decolorization rates of the two dye wastewater. And on the other, the pH value of the wastewater could also influence the performance of the coagulants. Under acid conditions, too much  $H^+$  could neutralize OH of the coagulants. This was not propitious for the stable presence of the coagulant, thereby the coagulation performance reduced. While, the pH value of direct fast claret dye wastewater (pH 5.55) was lower than that of direct sky blue (pH 7.49), so its decolorization rate was lower.

Fig. 6 also shows that the coagulation performance of Ce-PFS was superior to PFS, and the coagulation performance of Ce-PFS(A) was better than the others. Combined with the analysis result of 3.1.2, 3.1.4, and 3.2.1, it was due to that  $Ce^{3+}$  could improve the performance of the coagulant, and the less Ce-OH-Fe resulted in the worse performance.

### 3.2.3. Effect of coagulant dosage on decolorization rate

Fig. 7 illustrates the coagulation performance of Ce-PFS(A) ( $r = 0.6\%$ ) with different coagulant dosages. It was evident that the coagulation efficiency was affected by the amount of coagulant. When the dosage was not more than 75 mg/L, the decolorization rate increased markedly with the dosage of the coagulant. At the dosage of 75 mg/L, the decolorization rate reached up to 98%. However, it was reduced because of too large dosage. This was because that it was difficult to form the flocs due to the poor adsorption of the coagulating agent on the surface of the colloidal particles when the dosage was too little [29]. And because of the redundant coagulating agent, the colloidal particles would contain opposite charge which

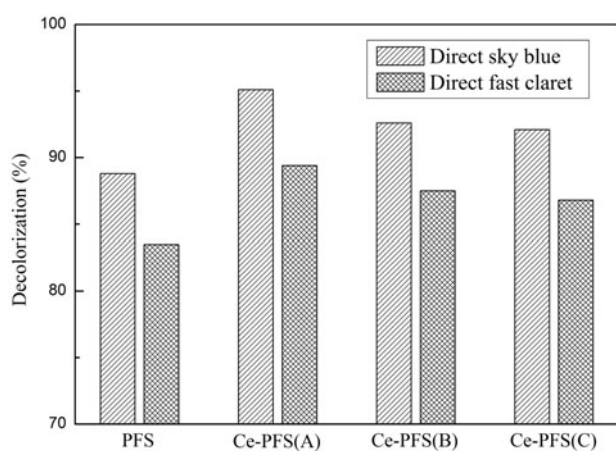


Fig. 6. Performance of the coagulants for treating different dye wastewater.

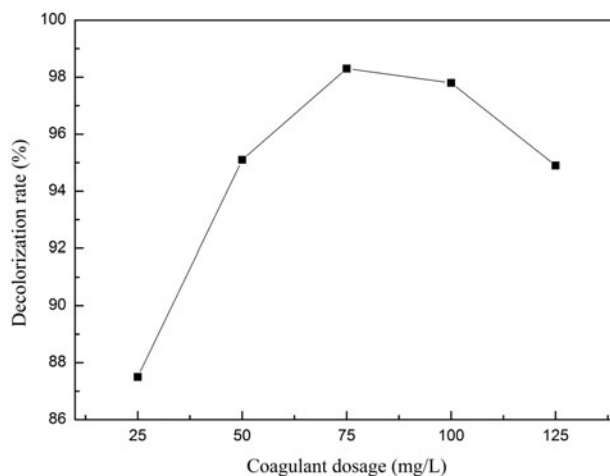


Fig. 7. Performance of Ce-PFS(A) ( $r = 0.6\%$ ) with different coagulant dosages.

caused the re-stability happening [30]. At the same time, the color of coagulant itself under high dosage could influence the light absorption of the solution.

#### 4. Conclusions

The conclusions drawn from this research are as follows:

- (1) PFS and a series of composite coagulants Ce-PFS were prepared through oxidation of  $\text{NaClO}_3$  with  $\text{FeSO}_4 \cdot 7\text{H}_2\text{O}$  as the raw material and  $\text{Ce}(\text{NO}_3)_3 \cdot 6\text{H}_2\text{O}$  as the modifier.
- (2) The analysis of FTIR, UV spectra, and XRD indicated that the reactions between  $\text{Ce}^{3+}$  and PFS were not simplex physical blends, but the new bond Ce–OH–Fe was formed between them. Additionally, the molecular weight of the coagulant and the accumulation charge of the single particle were increased after the addition of  $\text{Ce}^{3+}$ .
- (3) According to the analysis of Fe species in coagulant,  $\text{Ce}^{3+}$  promoted the conversion of Fe (a) to Fe(b) and Fe(c), and Fe(b) reached the maximum value when  $r = 0.6\%$ .
- (4) The coagulation experiments suggested that Ce-PFS showed better performance than PFS. When the molar ratio of Ce/Fe was 0.6%, the dosage was 75 mg/L, the decolorization rate of Ce-PFS(A) for treating direct sky blue could reach up to 98%. Meanwhile, the decolorization rate of direct sky blue was higher than that of direct fast claret dye wastewater under the same condition.

#### References

- [1] J.C. Wei, B.Y. Gao, Q.Y. Yue, Y. Wang, Effect of dosing method on color removal performance and flocculation dynamics of polyferric-organic polymer dual-coagulant in synthetic dyeing solution, *Chem. Eng. J.* 151 (2009) 176–182.
- [2] G.C. Zhu, H.L. Zheng, W.Y. Chen, W. Fan, P. Zhang, T. Tshukudu, Preparation of a composite coagulant: Polymeric aluminum ferric sulfate (PAFS) for wastewater treatment, *Desalination* 285 (2012) 315–323.
- [3] T. Leiviskä, J. Rämö, H. Nurmesniemi, R. Pöykiö, T. Kuokkanen, Size fractionation of wood extractives, lignin and trace elements in pulp and paper mill wastewater before and after biological treatment, *Water Res.* 43 (2009) 3199–3206.
- [4] L. Fan, T. Nguyen, F.A. Roddick, J.L. Harris, Low-pressure membrane filtration of secondary effluent in water reuse: Pre-treatment for fouling reduction, *J. Membr. Sci.* 320 (2008) 135–142.
- [5] M.F. Chong, K.P. Lee, H.J. Chieng, I.I. Syazwani Binti Ramli, Removal of boron from ceramic industry wastewater by adsorption–flocculation mechanism using palm oil mill boiler (POMB) bottom ash and polymer, *Water Res.* 43 (2009) 3326–3334.
- [6] Z.L. Yang, X.W. Lu, B.Y. Gao, Y. Wang, Q.Y. Yue, T. Chen, Fabrication and characterization of poly(ferric chloride)-polyamine flocculant and its application to the decolorization of reactive dyes, *J. Mater. Sci.* 49 (2014) 4962–4972.
- [7] P.A. Moussas, A.I. Zouboulis, Synthesis, characterization and coagulation behavior of a composite coagulation reagent by the combination of polyferric sulfate (PFS) and cationic polyelectrolyte, *Sep. Purif. Technol.* 96 (2012) 263–273.
- [8] M.H. Fan, S. Sung, R.C. Brown, T.D. Wheelock, F.C. Laabs, Synthesis, characterization, and coagulation of polymeric ferric sulfate, *J. Environ. Eng.* 128 (2002) 483–490.
- [9] W.P. Cheng, Comparison of hydrolysis/coagulation behavior of polymeric and monomeric iron coagulants in humic acid solution, *Chemosphere* 47 (2002) 963–969.
- [10] A.K. Verma, R.R. Dash, P. Bhunia, A review on chemical coagulation/flocculation technologies for removal of colour from textile wastewaters, *J. Environ. Manage.* 93 (2012) 154–168.
- [11] Z.P. King, D.Z. Sun, Treatment of antibiotic fermentation wastewater by combined polyferric sulfate coagulation, Fenton and sedimentation process, *J. Hazard. Mater.* 168 (2009) 1264–1268.
- [12] Y.B. Zeng, J.B. Park, Characterization and coagulation performance of a novel inorganic polymer coagulant—Poly-zinc-silicate-sulfate, *Colloids Surf., A* 334 (2009) 147–154.
- [13] Y.X. Zhao, B.Y. Gao, H.K. Shon, B.C. Cao, J.H. Kim, Coagulation characteristics of titanium (Ti) salt coagulant compared with aluminum (Al) and iron (Fe) salts, *J. Hazard. Mater.* 185 (2011) 1536–1542.
- [14] N.D. Tzoupanos, A.I. Zouboulis, Y.C. Zhao, The application of novel coagulant reagent (polyaluminum silicate chloride) for the post-treatment of landfill leachates, *Chemosphere* 73 (2008) 729–736.
- [15] Y. Zhao, L.Y. Zhang, F. Ni, B. Xi, X.F. Xia, X.J. Peng, Z.K. Luan, Evaluation of a novel composite inorganic coagulant prepared by red mud for phosphate removal, *Desalination* 273 (2011) 414–420.
- [16] N.D. Tzoupanos, A.I. Zouboulis, Preparation, characterisation and application of novel composite coagulants for surface water treatment, *Water Res.* 45 (2011) 3614–3626.
- [17] P.A. Moussas, A.I. Zouboulis, A new inorganic–organic composite coagulant, consisting of polyferric sulphate (PFS) and polyacrylamide (PAA), *Water Res.* 43 (2009) 3511–3524.
- [18] A. Matilainen, M. Vepsäläinen, M. Sillanpää, Natural organic matter removal by coagulation during drinking water treatment: A review, *Adv. Colloid Interface Sci.* 159 (2010) 189–197.
- [19] H. Moriwaki, R. Koide, R. Yoshikawa, Y. Warabino, H. Yamamoto, Adsorption of rare earth ions onto the cell walls of wild-type and lipoteichoic acid-defective strains of *Bacillus subtilis*, *Appl. Microbiol. Biotechnol.* 97 (2013) 3721–3728.

- [20] J.C. Kuang, Effect of adding rare earths into iron-carbon micro electrolysis process on degradation of dyeing wastewater, *Adv. Mater. Res.* 1021 (2014) 25–28.
- [21] O.V. Grechin, P.R. Smirnov, Ion coordination in aqueous solutions of cerium nitrate from X-ray diffraction data, *Russ. J. Coord. Chem.* 41 (2015) 47–50.
- [22] P.A. Moussas, A.I. Zouboulis, A study on the properties and coagulation behaviour of modified inorganic polymeric coagulant-polyferric silicate sulphate (PFSiS), *Sep. Purif. Technol.* 63 (2008) 475–483.
- [23] M.M. Clark, P. Lucas, Diffusion and partitioning of humic acid in a porous ultrafiltration membrane, *J. Membr. Sci.* 143 (1998) 13–25.
- [24] Y. Zhang, S.Y. Guo, J.T. Zhou, C.Y. Li, G.D. Wang, Flue gas desulfurization by  $\text{FeSO}_4$  solutions and coagulation performance of the polymeric ferric sulfate by-product, *Chem. Eng. Process.* 49 (2010) 859–865.
- [25] H.M. Wang, X.B. Min, L.Y. Chai, Y.D. Shu, Biological preparation and application of poly-ferric sulfate flocculant, *Trans. Nonferrous Met. Soc. China* 21 (2011) 2542–2547.
- [26] R. Scholz, N.V. Chukanov, L.A.D. Filho, D. Atencio, L. Lagoeiro, F.M. Belotti, M.L.S.C. Chaves, A.W. Romano, P.R. Brandao, D.I. Belakovskiy, I. Pekov, Cesarferreiraite,  $\text{Fe}^{2+}\text{Fe}^{23+}(\text{AsO}_4)_2(\text{OH})_2 \cdot 8\text{H}_2\text{O}$ , from Eduardo mine, Conselheiro Pena, Minas Gerais, Brazil: Second arsenate in the laueite mineral group, *Am. Mineral.* 99 (2014) 607–611.
- [27] H.L. Zheng, D.J. Peng, X.H. Huang, H. Liu, Study on the spectrum of the flocculent conformation of polymer ferric sulfate flocculants, *Spectrosc. Spect. Anal.* 27 (2007) 2480–2483 (in Chinese).
- [28] J. Chen, X.T. Rao, X.H. Jiang, *Spectrum Analysis*, University of Electronic Science and Technology Press, Chengdu, 2003 (in Chinese).
- [29] T. Sun, C.H. Sun, G.L. Zhu, X.J. Miao, C.C. Wu, S.B. Lv, W.J. Li, Preparation and coagulation performance of poly-ferric-aluminum-silicate-sulfate from fly ash, *Desalination* 268 (2011) 270–275.
- [30] Y. Suzuki, T. Maruyama, Removal of emulsified oil from water by coagulation and foam separation, *Sep. Sci. Technol.* 40 (2005) 3407–3418.